# Constructing conditional symmetry in a chaotic map

Chunbiao Li[1, 2 a)], Yongxin Li[1, 2], Wanning Yu[1, 2], Irene Moroz[3], and Christos Volos[4]

[1]*School of Artificial Intelligence, Nanjing University of Information Science & Technology, Nanjing 210044, China*

[2]*School of Electronic and Information Engineering, Nanjing University of Information Science & Technology, Nanjing 210044, China*

[3]*Mathematical Institute, University of Oxford, Oxford OX2 6GG, UK*

[4]*Laboratory of Nonlinear Systems, Circuits & Complexity (LaNSCom), Department of Physics, Aristotle University of Thessaloniki, 54124 Thessaloniki, Greece*

## ABSTRACT

Chaotic systems with conditional symmetry have been proven to be greatly efficient for chaotic outcomes and regulation. Offset boosting hidden in an absolute value function not only provides a new possibility for polarity balance but also returns suitable feedback for chaos generation. It has been verified that a conditional symmetric system exhibits two coexisting oscillations with opposite polarities along some specific dimensions and with directly-controlled offset by a constant. In a chaotic map, offset boosting shows its difference from the continuous system, where the left hand of a discrete system does not have the Dimension of Variable Differentiation (DVD), and the Built-in Polarity Reversal (BPR) can be embedded simultaneously for a double-petal attractor bringing different polarity feedback within the odd or even subsequence and thus modifying the symmetrical pairs of phase orbits according to two separate subsequences. Consequently, the construction of conditional symmetry in a chaotic map has its special strategy. In this paper, all the above unique characteristics are taken into consideration for the map construction with conditional symmetry.

---

a) Corresponding author, E-mail address: goontry@126.com; chunbiaolee@nuist.edu.cn

**Keywords:** Chaotic map, offset boosting, conditional symmetry.

## 1. Introduction

Chaos, for its unique wideband property and butterfly effect, has been proven to have great potential in chaos-based applications [1-3]. Multistable chaotic systems have attracted great attention for their more available outcomes and flexible initial condition-oriented controllability [4-6]. Along with the development of geometric control within chaos [7-8] and offset-dominated dynamics [9-11], the offset factor has been regarded as powerful for multistability design. In a chaotic system, a single strange attractor in phase space can be doubled in different ways, through symmetry [12-13] or conditional symmetry [14-15]. Or, it can be self-reproduced forming a one-dimensional chain [16-17] or multi-dimensional lattice [18-19]. Attractor growth has been observed in many nonlinear memristive systems for the closely arranged coexisting attractors, where the system crosses various regions of chaos under the inner calculation noise until it exceeds the limitation of hardware [20]. All these offset-dominated multistabilities should reappear in a discrete map. However, the absence of Dimension of Variable Differentiation (DVD) makes it unclear for polarity reverse and recovery [21].

Recently, the construction of chaotic discrete maps has become more and more popular for its easy production, where chaotic sequences are employed for controlling resources in chaos-based applications rather than from those chaotic signals. Chaotic maps with conditional symmetry have been discovered occasionally when new nonlinear feedback is introduced [22]. Undoubtedly, both the offset boosting realization and the offset-dominated polarity regulation in a discrete map are different from those in a continuous system, which needs further clarifying. Furthermore, the embedded polarity reverse from a direct variable self-feedback can win extra regions for double-petal phase trajectories. In this paper, the inner mechanism of polarity regulation is exhaustively explored, by which one can construct a chaotic map with conditional symmetry for outputting coexisting pairs of attractors. In section 2, the recovery of DVD is employed for conditional symmetry, conditional reflection symmetry is obtained by one-dimensional offset boosting with a polarity reverse from a variable, and conditional

rotational symmetry is also obtained by two-dimensional offset boosting. In section 3, the inherent polarity reverse is considered for the recovery of polarity balance and consequently the conditional symmetry obtains the flexibility of adjustable-interval four-petal output. In section 4, circuit realization based on the digital platform is employed to show the effectiveness of conditional symmetry construction. In the last section, conclusions are drawn.

## 2. Polarity balance from the recovery of DVD for conditional symmetry

For a difference equation, the polarity reverse of a variable is independent of the difference components, which is different from the case in a differential equation. We can see that, in a discrete map, if the polarity of variable $x$ gets polarity reversed, it means that all the sequences like $x_n$ and $x_{n+1}$ become sign reversed, *i.e.*, $x_n \to -x_n$ and $x_{n+1} \to -x_{n+1}$, it turns out that the polarity of $(x_{n+1} - x_n)$ gets polarity reversed, but in a differential equation, the polarities of $x$ and $\dot{x}$ are locked together. Therefore, in a difference equation, three items should be considered for polarity balance rather than two items in a differential equation.

[**Remark 1**] For maintaining the fundamental dynamics of a system, the desired transformation should obey the basic law of polarity balance. In a discrete map, the polarity imbalance induced by the polarity reversal of any of the variables can be recovered by the offset boosting of any other of the variables since there are some functions return a polarity reversal on the right-hand side for the reason of offset boosting, which does not revise the polarity of the left-hand side of the map.

[**Remark 2**] For a discrete map $X(n+1) = F(X(n)) = (f_1(X(n)), f_2(X(n)), \dots, f_N(X(n)))$ $(X = (x_1, x_2, \dots, x_N))$, if the polarity balance comes both from variable polarity reverse and offset boosting such as $x_{i_1}(n+1) = -x_{i_1}(n+1), x_{i_1}(n) = -x_{i_1}(n), x_{i_2}(n+1) = -x_{i_2}(n+1), x_{i_2}(n) = -x_{i_2}(n), \cdots, x_{i_k}(n+1) = -x_{i_k}(n+1), x_{i_k}(n) = -x_{i_k}(n), x_{j_1}(n+1) = x_{j_1}(n+$

$1) + d_{j_1}, x_{j_1}(n) = x_{j_1}(n) + d_{j_1}, x_{j_2}(n+1) = x_{j_2}(n+1) + d_{j_2}, x_{j_2}(n) = x_{j_2}(n) +$ $d_{j_2}, \cdots, x_{j_l}(n+1) = x_{j_l}(n+1) + d_{j_l}, x_{j_l}(n) = x_{j_l}(n) + d_{j_l}, x_i(n+1) = x_i(n+$ $1), x_i(n) = x_i(n),$ , (here $1 \le i_1, \cdots, i_k \le N$ , $1 \le j_1, \cdots, j_l \le N$ , $, i_1, \cdots, i_k$ and $j_1, \cdots, j_l$ are not identical, $i \in \{1,2, \ldots, N\} \backslash \{i_1, \cdots, i_k, j_1, \cdots, j_l\}$), the map $X(n+1) = F(X(n))$ $(X = (x_1, x_2, \ldots, x_N))$ can be defined as one of *l*-dimensionally conditional symmetry since the polarity balance depends on *l*-dimensional offset boosting.

For conditional symmetry, the polarity balance should come from both the variable and from the offset-boosting-involved function, as shown in Fig. 1. As we know, the polarity reverse triggered by offset boosting typically comes from an absolute value function or a trigonometric function. Unlike the case in the continuous differential system, in a difference map, the offset boosting in any of the dimensions brings an extra constant on the left-hand side of the equation, which needs the same constant on the right to cancel it. This means that, if the variable $x_i$ needs the offset boosting for returning the polarity balance, both the new state $x_{i(n+1)}$ and the old state $x_{i(n)}$ should appear on both sides of the equation simultaneously. This means that the DVD should be kept for the construction of conditional symmetry, which leads to full-sequence conditional symmetry. However, BPR in a map typically gives a double-petal attractor from the odd and even subsequences, any of which could get polarity balance from its own offset-aided polarity reversal, and thus here comes up a new region of subsequence conditional symmetry.

Here, in the following, we try to demonstrate this using the absolute value function. For a multiple-dimensional map, the polarity reverse from the system variables could bring different regimes of symmetry, such as reflectional symmetry, rotational symmetry, and inversion symmetry. In the following, we try to give examples of this direction.

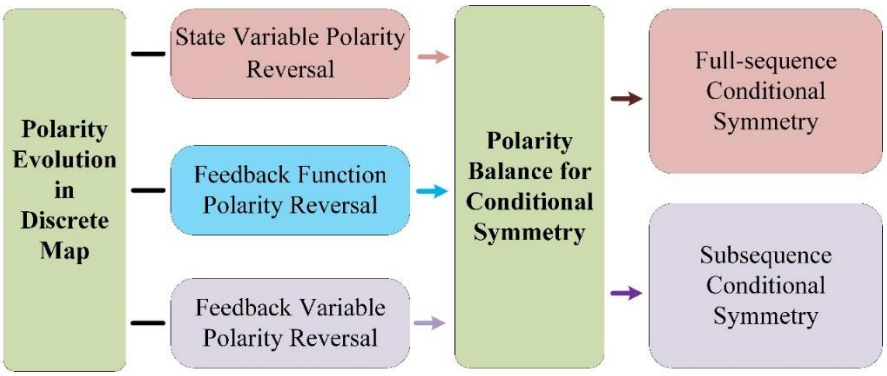



Fig. 1. Polarity balance for conditional symmetry.

### 2.1 Conditional reflectional symmetry from a single step of offset boosting

We consider the polarity balance induced by the variable polarity revised and offset boosted in any of the dimensions in the equation. Take the original Holmes cubic map [23] for example,

$$\begin{cases} x_{n+1} = y_n, \\ y_{n+1} = -ax_n + by_n - y_n^3. \end{cases} \tag{1}$$

We know that when $a$ = 0.2, $b$ = 2.77, system (1) exhibits chaos with Lyapunov exponents (0.581462, -2.19219). The coexistence of $y_{n+1}$ and $y_n$ gives the chance for offset boosting bringing an extra polarity reverse to cancel the polarity revision from a system variable. Therefore, we need to change the feedback in the second equation of system (1) accordingly. An easy way to shield the polarity change is to apply an absolute value operation.

**[Theorem 2.1]** The derived equation could be equipped for offset-boosting-regulated conditional reflection symmetry with respect to the $x$ dimension by introducing a nonmonotonic function $F(y_n)$,

$$\begin{cases} x_{n+1} = ay_n \\ y_{n+1} = y_n + b\,|\,x_n\,| - c\,|\,y_n\,| \end{cases} \tag{2}$$

**[Proof 2.1]** If $x_{n+1} \to -x_{n+1}$, $x_n \to -x_n$, $y_{n+1} \to y_{n+1}$, $y_n \to y_n$, the polarity balance of the first dimension of Eq. (2) is destroyed because of the polarity invariance in the variable $y_n$ and $y_{n+1}$, while the polarity balance in the second dimension $y_{n+1}$ is preserved. However, offset boosting in the dimension of $y$ can win an extra polarity

reversal and restore the polarity balance in the first dimension if a suitable function is introduced. Suppose $y_n \rightarrow F(y_n)$, since $F(y_n)$ is nonmonotonic, if $y_{n+1} \rightarrow y_{n+1} + d_{ob}$, $y_n \rightarrow y_n + d_{ob}$ makes $F(u_n) = F(y_n + d_{ob}) = -F(y_n)$, the variable substitution $x_{n+1} \rightarrow -x_{n+1}$, $x_n \rightarrow -x_n$, $y_{n+1} + d_{ob} \rightarrow y_{n+1} + d_{ob}$, $y_n + d_{ob} \rightarrow y_n + d_{ob}$ will restore the polarity balance in the following equation,

$$\begin{cases} x_{n+1} = aF(y_n) \\ y_{n+1} = y_n + b\,|\,x_n\,| - c\,|\,F(y_n)\,| \end{cases} \tag{3}$$

which proves that map (2) can be transformed into the map (3) with conditional reflection symmetry by a special nonmonotonic function $F(y_n)$.

Taking a function substitution, like $F(y_n) = |y_n| - d$, with the original state variable $y_n$ for polarity revision, two coexisting phase orbits with conditional symmetry will appear. Note that, here an independent state variable $y_n$ should be preserved for offset balance in the second dimension. When $a = 1.09$, $b = 1.101$, $c = 1.2$, and $(x_0, y_0) = (0.3, 0.3)$, we find the map (2) gives chaos with Lyapunov exponents (0.1784, -0.0059), whose phase orbit and discrete sequences are plotted in Fig. 2. Under the same parameter combinations, map (3) gives coexisting conditional symmetric attractors, as shown in Fig. 3 (a)(b). Different offset constants regulate the distance between two coexisting attractors. All coexisting attractors share the same Lyapunov exponents of (0.1806, -0.0055) when the offset parameter $d$ varies in [9, 23], as shown in Fig. 3 (c)(d). Each branch of the bifurcation contains two bands representing the composite structure of attractors. Basins of attraction for two coexisting symmetrical attractors of the map (3) are displayed in Fig. 4. The green area represents the green attractor, and the purple area represents the purple attractor. Two regions of the basin of attraction are clearly distinguished by the offset of two attractors.

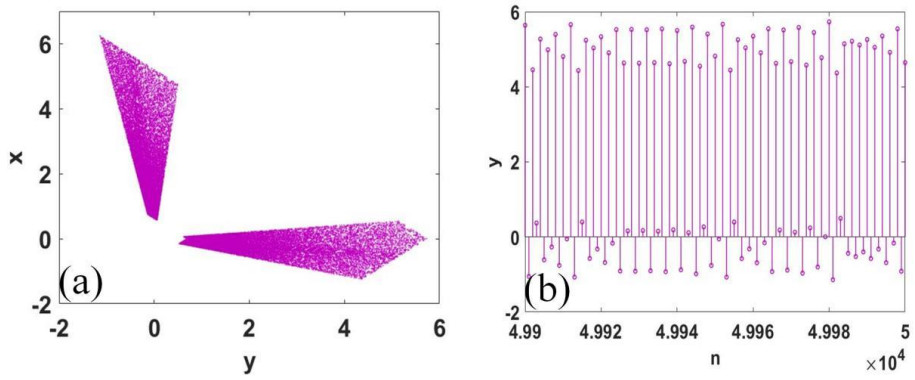



Fig. 2. Typical dynamical oscillation of the map (2) with $a$ = 1.09, $b$ = 1.101, $c$ = 1.2, and ($x_0$, $y_0$) = (0.3, 0.3): (a) phase orbits, (b) discrete sequences.

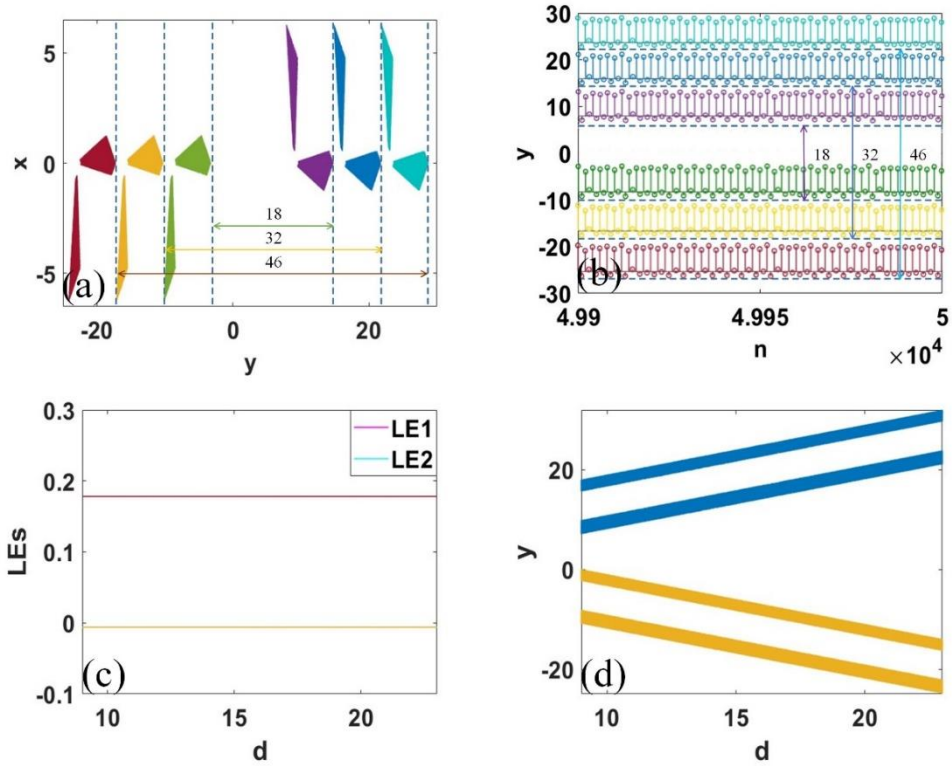



Fig. 3. Offset-regulated conditional symmetry in the map (3) with $a$ = 1.09, $b$ = 1.101, $c$ = 1.2: (a) phase orbits, (b) chaotic sequences, (c) unified Lyapunov exponents, (d) coexisting bifurcations, dark blue: IC = (0.3, 0.3 + $d$), yellow: IC = (– 0.3, 0.3 – $d$). Here $d$ is set to 9, 16, and 23 respectively for adjusting the offset of coexisting attractors, purple: IC = (0.3, 9.3), green: IC = (–0.3, –8.7), dark blue: IC = (0.3, 16.3), yellow: IC = (–0.3, -15.7), light blue: IC = (0.3, 23.3), brown: IC = (–0.3, –22.7).

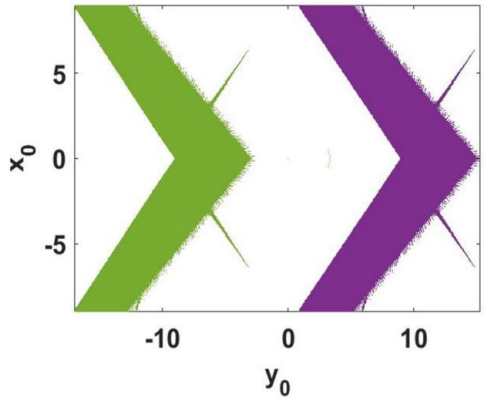



Fig. 4. Basins of attraction for two coexisting conditional symmetrical attractors of the map (3) with $a$ = 1.09, $b$ = 1.101, $c$ = 1.2.

### 2.2 Conditional rotational symmetry from a single step of offset boosting

For rotational symmetry, the dimension of the discrete map should be at least three. In this case, typically we need revise the map with higher-dimensional feedback by introducing a new dimension.

**[Theorem 2.2]** The discrete map (4) can be transformed into a system with conditional rotational symmetry with respect to the dimensions of $x$ and $z$ by introducing a nonmonotonic function $F(y_n)$.

$$\begin{cases} x_{n+1} = ay_n \\ y_{n+1} = y_n + b\,|\,x_n\,| - c\,|\,y_n\,| \\ z_{n+1} = ez_n + y_n \end{cases} \tag{4}$$

**[Proof 2.2]** If $x_{n+1} \to -x_{n+1}$, $x_n \to -x_n$, $y_{n+1} \to y_{n+1}$, $y_n \to y_n$, $z_{n+1} \to -z_{n+1}$, $z_n \to -z_n$,the polarity balance of the first and last dimension of Eq. (4) are destroyed for the fixed polarity of the variable $y_n$ and $y_{n+1}$, while the polarity balance in the second dimension $y_{n+1}$ keeps preserved. This time, offset boosting in the dimension of $y$ can restore the polarity balance in the first and last dimension if a suitable function is introduced. Suppose $y_n \to F(y_n)$, since $F(y_n)$ is nonmonotonic, if $y_{n+1} \to y_{n+1} + d_{ob}$, $y_n \to y_n + d_{ob}$ makes $F(u_n) = F(y_n + d_{ob}) = -F(y_n)$, the variable substitution $x_{n+1} \to -x_{n+1}$, $x_n \to -x_n$, $y_{n+1} + d_{ob} \to y_{n+1} + d_{ob}$,

$y_n + d_{ob} \to y_n + d_{ob}$ and $z_{n+1} \to -z_{n+1}$, $z_n \to -z_n$ will obtain the polarity balance in the following equation,

$$\begin{cases} x_{n+1} = aF(y_n) \\ y_{n+1} = y_n + b\,|\,x_n\,| - c\,|\,F(y_n)\,| \\ z_{n+1} = ez_n + F(y_n) \end{cases} \tag{5}$$

which proves that map (4) can be transformed into the map (5) with conditional rotational symmetry by a special nonmonotonic function $F(y_n)$.

When $a$ = 1.09, $b$ = 1.101, $c$ = 1.2, $e$ = 0.1, ($x_0$, $y_0$, $z_0$) = (0.3, 0.3, 0.3), the map (4) is chaotic with Lyapunov exponents of (0.1825, 0, –2.3044), whose phase orbit and discrete sequences are plotted in Fig. 5. Select the function $F(y_n) = |y_n| - d$, it is found that if the polarities of $x$ and $z$ get reversed, the operation of offset boosting within the dimension of $y_n$ brings an extra polarity reverse to recover the polarity balance leading to conditional rotational symmetry [14]. Set $a$ = 1.09, $b$ = 1.101, $c$ = 1.2, $e$ = 0.1, ($x_0$, $y_0$, $z_0$) = (0.3, 0.3, 0.3), the map (5) is chaotic with Lyapunov exponents of (0.1825, 0, –2.3044), whose phase orbit and dynamical evolvements are plotted in Fig. 6.

Note that in the dimension with offset revised, the corresponding DVD should be maintained. The distance between two coexisting attractors is regulated by the offset constant, as shown in Fig. 6(a) and (b), where the polarity reverses of $x$ and $z$ under the offset boosting of $y$ are clearly seen. The constant in the above absolute function is employed for modifying the distance between two coexisting attractors with almost unified set of Lyapunov exponents, as shown in Fig. 6(c) and (d). The details of the polarity revision of $x$ and the offset revision with the variable of $y$ are clearly shown in Fig. 6(e) and (f).

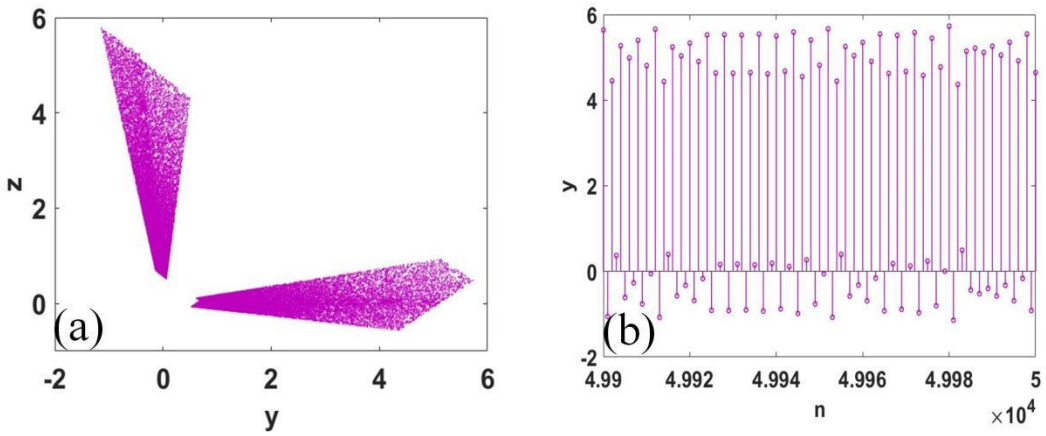



Fig. 5. Typical dynamical oscillation of the map (4) with $a$ = 1.09, $b$ = 1.101, $c$ = 1.2, $e$ = 0.1, ($x_0$, $y_0$, $z_0$) = (0.3, 0.3, 0.3): (a) phase orbits, (b) discrete sequences.

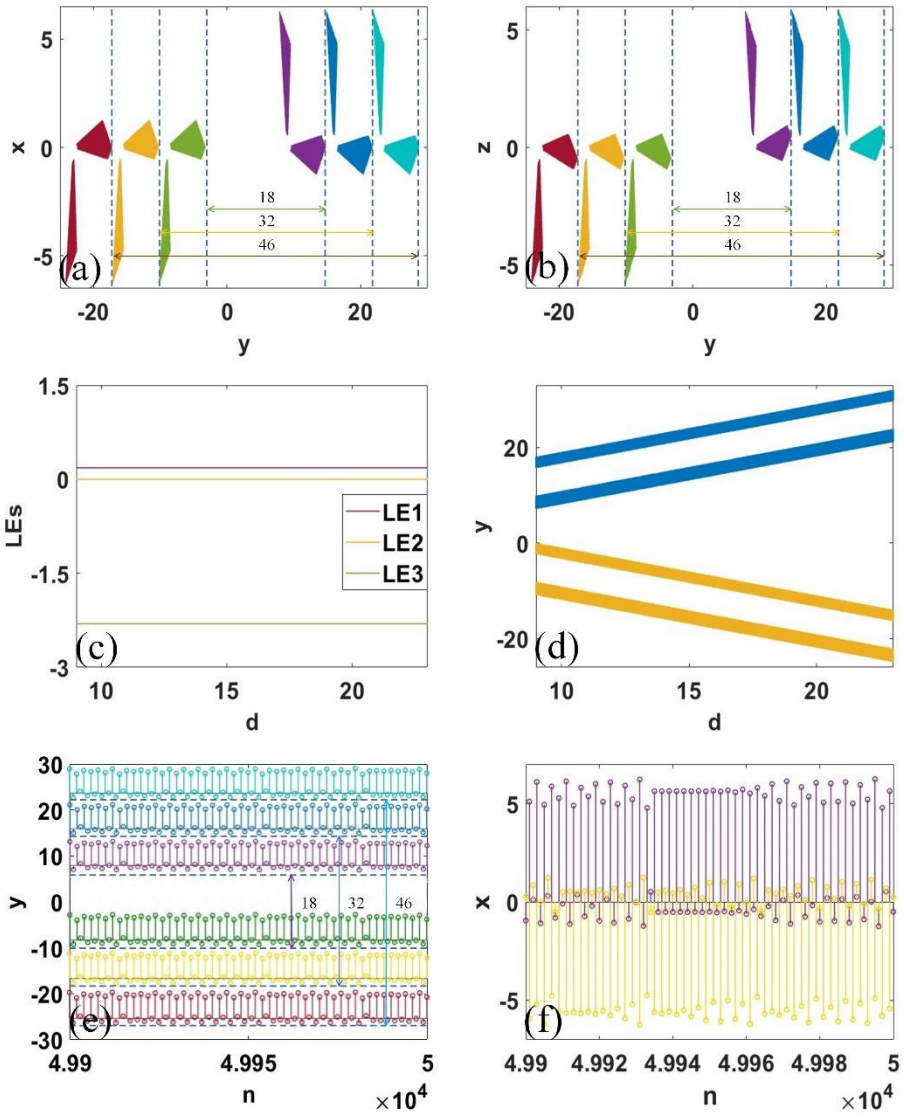


Fig. 6. The feature of conditional symmetry in the map (5) with $a$ = 1.9, $b$ = 1.101, $c$ = 1.2, $e$ = 0.1 under different initial conditions, here $d$ is set to 9, 16, 23 respectively, purple: IC = (0.3, 9.3, 0.3), green: IC = (–0.3, –8.7, 0.3), dark blue: IC = (0.3, 16.3, 0.3), yellow: IC = (–0.3, –15.7, 0.3), light blue: IC = (0.3, 23.3, 0.3), brown: IC = (–0.3, –22.7, 0.3): (a) phase trajectories in $y$-$x$ plane, (b) phase trajectories in $y$-$z$ plane, (c) unified Lyapunov exponents, (d) symmetric bifurcations, dark blue: IC = (0.3, 0.3 + $d$, 0.3), yellow: IC = (–0.3, 0.3–$d$, 0.3), (e) $y$-dimensional discrete sequences, (f) $x$-dimensional discrete sequences.

### 3. Built-in polarity reversal for conditional symmetry

In a discrete equation, the dimension of variable differentiation can be destroyed with the embedded synchronized polarity reversal. This time, the polarity balance from the offset boosting with the corresponding variable could be destroyed accordingly. As we noticed, the polarity of the variable with offset boosting is maintained for the fixed DVD. But if the DVD is broken by the built-in polarity reversal, the polarity reversal could be compensated and recovered also from the substitution of the absolute value function. Here the coexistence of the reverse polarity in the dimension with offset boosting gives the flexibility of variable-reverse iteration. This time, since the offset boosting within the absolute value function for the polarity balance is based on the initial condition, the hidden offset revision does not destroy the polarity balance.

Consider the map,

$$\begin{cases} x_{n+1} = ay_n \\ y_{n+1} = -y_n + b\,|\,x_n\,| - cy_n^2 \end{cases} \tag{6}$$

For parameter values: $a$ = 1.145, $b$ = -1, $c$ = 1, $(x_0, y_0)$ = (0.3, 0.3), the map (6) is chaotic with Lyapunov exponents of (0.1959, –1.0099). Typical phase orbits and corresponding chaotic sequences are plotted in Fig. 7. This time, map (6) gives a classic double-petal attractor, one petal is from the odd sequence and the other one is from the even sequence.

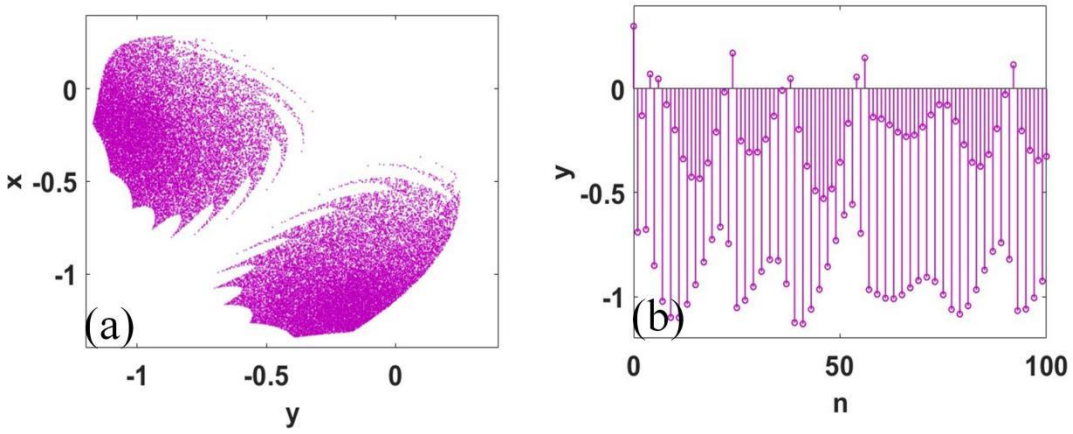



Fig. 7. Typical dynamical oscillation of the map (6) with $a$ = 1.145, $b$ = -1, $c$ = 1, ($x_0$, $y_0$) = (0.3, 0.3): (a) phase orbits, (b) discrete sequences.

Here the single polarity reverse of $y$ in the second dimension disturbs the iteration of itself rather than that of $x$, which leads to a double-petal of attractor for indirect iteration. The influence of the feedback from $-y_n$ on the new state of $y_{n+1}$ can be divided to be two subsequences of odd and even. Two subsequences can obtain their own polarity balances leading to conditional symmetry. One routine for odd sequence is from the transformation of $x_{2m+1} \to -x_{2m+1}$, $x_{2m-1} \to -x_{2m-1}$, $y_{2m+1} + d_{ob1} \to y_{2m+1} + d_{ob1}$, $y_{2m-1} + d_{ob1} \to y_{2m-1} + d_{ob1}$, and the other one for even sequence is from the transformation of $x_{2m+2} \to -x_{2m+2}$, $x_{2m} \to -x_{2m}$, $y_{2m+2} + d_{ob2} \to y_{2m+2} + d_{ob2}$, $y_{2m} + d_{ob2} \to y_{2m} + d_{ob2}$ ( here $m \geq 1$).

Therefore, offset-aided polarity balance under the built-in polarity reverse hidden in $y_{n+1}$+$y_n$ as appear in Eq.(6) can be divided into two subsequences. In other words, the offset happens in the absolute function based on the constant $d$ can balance the polarity reverse either for the odd subsequence or for the even subsequence. Then, the iteration of $y_{n+1} + y_n$ is just like a knife cutting the whole attractor into two petals driving the conditional symmetry towards to different parts in the attractor.

Introducing the function $F(y_n) = |y_n| - d$ to the above equation,

$$\begin{cases} x_{n+1} = aF(y_n) \\ y_{n+1} = -y_n + b\,|\,x_n\,| - cF^2(y_n) \end{cases} \tag{7}$$

set $a = 1.145$, $b = -1$, $c = 1$, $d = 2$, $(x_0, y_0) = (0.3, 0.3)$, the map (7) is chaotic with slightly revised set of Lyapunov exponents of (0.0964, 0.0391).

Coexisting attractors and the properties of evolution are shown in Fig. 8. Comparing the bifurcation diagrams of systems (3) and (7) from the plots shown in Fig. 3(d) and Fig. 8(d), we can see that this time the polarity reverse of the variable $y_n$ with the offset is also different, one is like reverse-shifting, the other is just like shifting-reverse. The former double petals clicked together, while the latter double petals correspond to two subsequences of odd and even. Basins of attraction for two coexisting conditional symmetrical attractors of the map (7) are plotted in Fig. 9. The green area is for the green attractor, and the purple area represents the purple one. Comparing the basins of attraction in systems (3) and (7) from the plots shown in Fig. 4 and Fig. 9, the basins of the coexisting attractors are also different. For the former case, the basin shows clear offset boosting while for the latter case, the basin shows the embedded fractal structure. From this view, the offset boosting for conditional symmetry, the former one is like a conjoined infant but the latter two petals are like twins.

Further demonstration of the influence due to the offset by the parameter and the initial condition are shown in Figs. 10-11. Here we can see clearly both the odd subsequence and the even one have their own corresponding conditional symmetric petals. In Fig. 10, green petal is from the even subsequence of map (7), two green petals are from the combinations of $x_{2m}$ with polarity reversal and $y_{2m}$ with offset boosting. When the petal attractor moves from the first quadrant (positive area) to the third quadrant (negative area), the offset in the dimension of $y$: $d_{ob2}$ = -4. But two red petals corresponding to $x_{2m-1}$ with polarity reversal and $y_{2m-1}$ with offset boosting move in opposite direction. The same-direction shifts of petal attractor correspond to opposite combinations of initial condition. Lyapunov exponents of conditional symmetry in the map (7) are shown in Fig. 12. Lyapunov exponents from the even and odd iterations are

almost the same and only exhibit slightly waving according to the offset parameter.

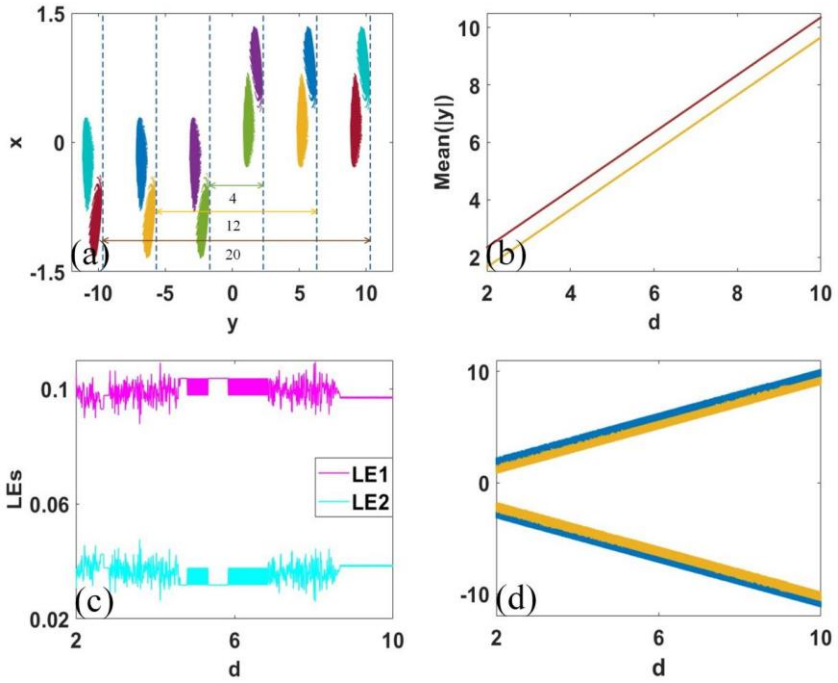



Fig. 8. The feature of conditional symmetry in the map (7) with $a$ = 1.145, $b$ = -1, $c$ = 1 under different initial conditions, here $d$ is set to 2, 6, 10 respectively, (a) phase orbits, purple: IC = (0.3, 2.3), green: IC = (–0.3, -1.7), dark blue: IC = (0.3, 6.3), yellow: IC = (–0.3, -5.7), light blue: IC = (0.3, 10.3), brown: IC = (–0.3, -9.7), (b) average variables of $|y|$, (c) unified Lyapunov exponents, (d) symmetric bifurcations, dark blue: IC = (0.3, 0.3 + $d$), yellow: IC = (-0.3, 0.3 - $d$).

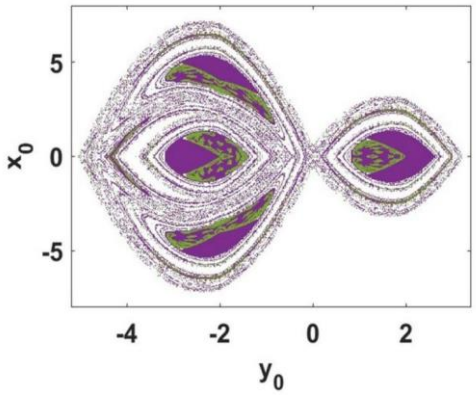



Fig. 9. Basins of attraction for two coexisting symmetrical attractors of map (7) with $a$ = 1.145, $b$ = -1, $c$ = 1.

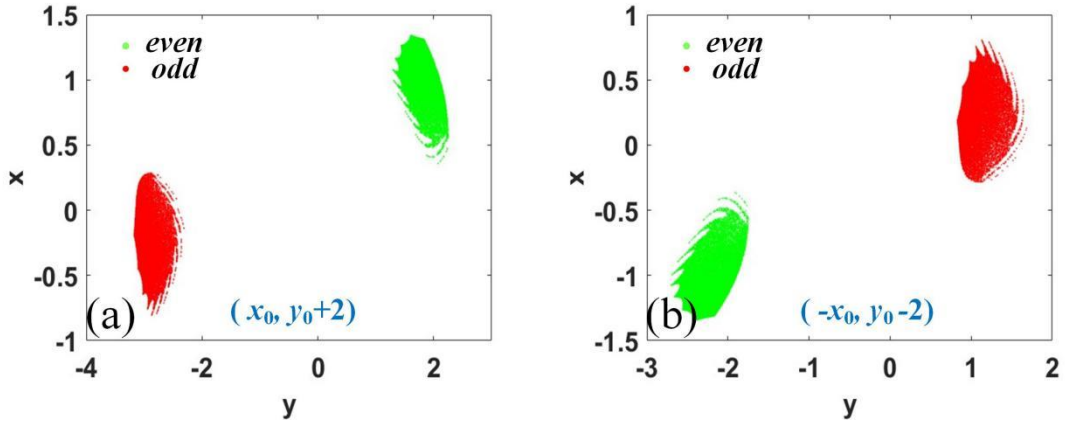



Fig. 10. Further demonstration of conditional symmetry in the map (7) with $a$ = 1.145, $b$ = -1, $c$ = 1, $d$ = 2 under different initial conditions, where the red attractor is from the odd subsequence, the green attractor is from the even subsequence: (a) IC = (0.3, 2.3), (b) IC = (–0.3, -1.7).

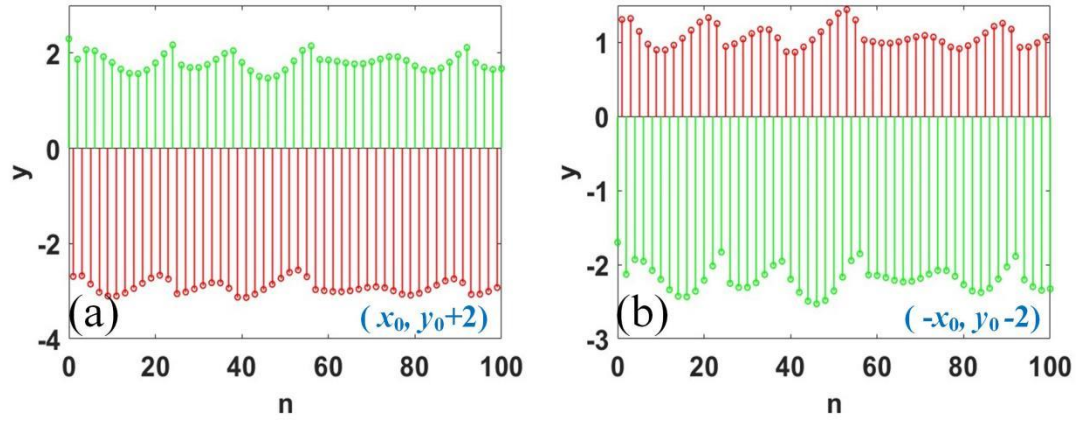



Fig. 11. Offset boosting of subsequences for conditional symmetry in the map (7) with $a$ = 1.145, $b$ = -1, $c$ = 1, $d$ = 2, where the odd sequence is red, the even sequence is green: (a) IC = (0.3, 2.3), (b) IC = (–0.3, -1.7).

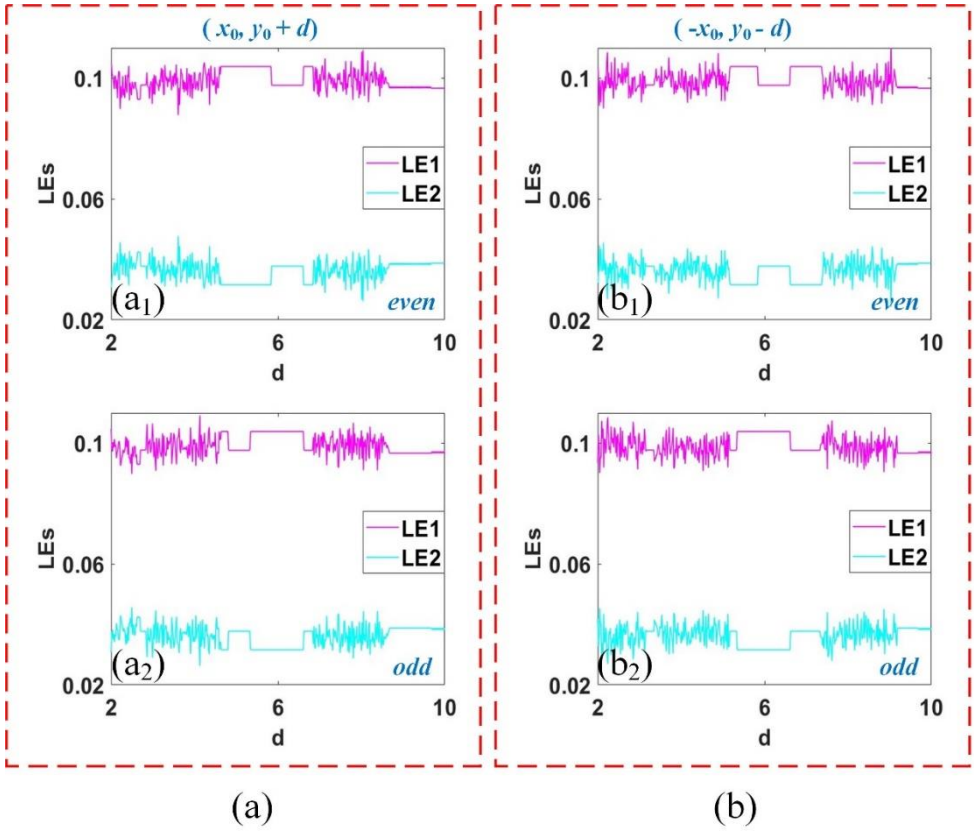



Fig. 12. Lyapunov exponents of conditional symmetry in map (7) with $a$ = 1.145, $b$ = -1, $c$ = 1, and $d$ = 2 under different initial conditions, where (a1)-(b1) come from even subsequence and (a2)-(b2) come from odd subsequence: (a) IC = (0.3, 2.3), (b) IC = (–0.3, –1.7).

## 4. Digital implementation bases on the platform of RISC-V

The calculation and output of the chaotic map above can be shown on the platform of RISC-V type of microcontroller CH32V307. The CH32V307 shares the 32-bit RISC-V instruction set and architecture, operating at a maximum frequency of 144MHz, with 256KB of Flash and 64KB of SRAM. It supports the floating-point operations accelerating computation for mapping. Moreover, the CH32V307 has two sets of 12-bit DAC converters, facilitating the conversion of chaotic digital signals into analog voltage. Those outputs, ranging between 0 and 4095, are written into the DAC_DORx register cyclically within the main program loop. The iteration process employs the resultant chaotic data as the initial value for the next cycle, until the predetermined number of iterations is reached. The analog voltage signals produced are then fed into

the $x/y$-axis inputs of an oscilloscope, revealing the phase trajectories on its display. The platform of digital circuit implementation is shown in Fig. 13. Offset-induced conditional symmetry is observed from the oscilloscope, shown in Figs. 14-15.

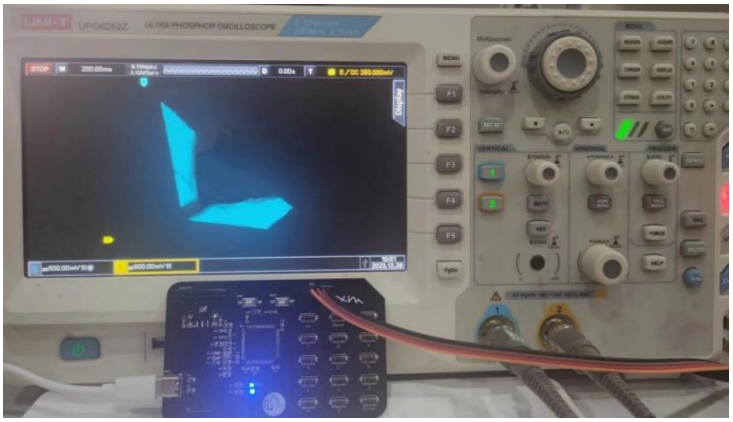


Fig.13. Digital circuit implementation of the map (3) with $a$ = 1.09, $b$ = 1.101, $c$ = 1.2 under IC = (0.3, 0.3).




Fig.14. Offset boosting-induced conditional symmetry in the map (3) observed in the oscilloscope with $a$ = 1.09, $b$ = 1.101, $c$ = 1.2 under different initial conditions, $d$ is set to 9, 16, 23 respectively, where purple: IC = (0.3, 9.3), green: IC = (–0.3, -8.7), dark blue: IC = (0.3, 16.3), yellow: IC = (–0.3, -15.7), light blue: IC = (0.3, 23.3), brown: IC = (–0.3, -22.7).




Fig.15. Offset boosting-induced conditional symmetry in the map (7) observed in the oscilloscope with $a$ = 1.145, $b$ = -1, $c$ = 1 under different initial conditions, $d$ is set to 2, 6, 10 respectively, where purple: IC = (0.3, 2.3), green: IC = (–0.3, -1.7), dark blue: IC = (0.3, 6.3), yellow: IC = (–0.3, -5.7), light blue: IC = (0.3, 10.3), brown: IC = (–0.3, -9.7).

## 5. Conclusion

When the polarity reverse comes both from the variable and the feedback function with offset-triggered polarity inversion, conditional symmetry can be obtained in a chaotic discrete map outputting two groups of chaotic flows with opposite polarities. Chaotic maps with conditional reflection symmetry and conditional rotational symmetry can be derived based on the selection and revision of the structure of chaotic maps. Here we define the variable as the conditional one, where the polarity reverse is from the offset-involved absolute value function rather than from itself. When the BPR is considered for additional polarity revise, here we can see two routines to the construction of conditional symmetry. Firstly, like in the continuous systems, the DVD of the conditional variable is traditionally protected in the same direction of evolution for obtaining the offset-independence. The coexisting conditional symmetric attractors of such class stand in phase space with clearly separated offset and can be extracted by the same-directional offset boosted initial conditions.

Secondly, totally different from those continuous systems, when the BPR is attached in the map, the DVD of the conditional variable could be obtained in the opposite direction of evolution resulting two petals of the attractor, which comes from the odd subsequence or even subsequence. This time, the original orbit of the map splits to double petals with the same Lyapunov exponents belonging to odd and even iterations. Each petal of the attractor has its own mirror attractor standing in phase space and can be controlled by the offset parameter with opposite directions. All the polarity reverse from the offset boosting in the feedback function can be balanced along with the offset selection of the initial condition and the variable polarity reversal.

Two mechanisms of conditional symmetry dominated by DVD and BPR are exhaustively explored based on the derived models of Holmes cubic map [23]. Three regimes of conditional symmetry are also classified including conditional reflectional symmetry from a single step of offset boosting, conditional rotational symmetry from a single step of offset boosting, and the subsequence conditional symmetry. Both of the full-sequence and subsequence conditional symmetry induced by the offset boosting output coexisting sequences with different polarities and average values, which brings great benefits to chaos applications. The engineering application of conditional symmetric map is a promising future direction for its dual outputs with two sets of unipolar signals.

**Acknowledgments**

This work was supported financially by the National Natural Science Foundation of China (Grant No.: 62371242).

**Data availability statement**

The data that support the findings of this study are available from the corresponding author upon reasonable request.

**Conflict of interest**

We declare that we have no known competing financial interests or personal relationships that could have appeared to influence the work reported in this paper.

## Author Contributions

**Chunbiao Li**: Conceptualization(lead); Formal analysis (equal); Writing – original draft (lead); Funding acquisition. **Yongxin Li**: Methodology (equal); Formal analysis (equal); Visualization (equal). **Wanning Yu**: Methodology (equal); Visualization (equal). **Irene Moroz:** Visualization (equal); Writing – review & editing (equal). **Christos Volos:** Visualization (equal); Writing – review & editing (equal).

## References


[1] Li B, Sun K, Wang H, et al. A delay-disturbance method to counteract the dynamical degradation of digital chaotic systems and its application. Chaos, Solitons & Fractals, 2024, 182: 114843.

[2] Chen X, Mou J, Cao Y, et al. Chaotic Multiple-Image Encryption Algorithm Based on Block Scrambling and Dynamic DNA Coding. International Journal of Bifurcation and Chaos, 2023, 33(16): 2350190.

[3] Liu W, Sun K, He S, et al. The parallel chaotification map and its application. IEEE Transactions on Circuits and Systems I: Regular Papers, 2023, 70(9): 3689-3698.

[4] Sriram G, Parastesh F, Natiq H, et al. Multistable ghost attractors in a switching laser system. Chaos: An Interdisciplinary Journal of Nonlinear Science, 2023, 33(11): 113119.

[5] Ali A M A, Sriram S, Natiq H, et al. A novel multi-stable sinusoidal chaotic map with spectacular behaviors. Communications in Theoretical Physics, 2023, 75(11): 115001.

[6] Zhang S, Zheng J, Wang X, et al. Multi-scroll hidden attractor in memristive HR neuron model under electromagnetic radiation and its applications. Chaos: An Interdisciplinary Journal of Nonlinear Science, 2021, 31(1): 011101.

[7] Wu Q, Hong Q, Liu X, et al. A novel amplitude control method for constructing nested hidden multi-butterfly and multiscroll chaotic attractors. Chaos, Solitons & Fractals, 2020, 134: 109727.

[8] Chai L, Liu J, Chen G, et al. Amplitude control and chaotic synchronization of a complex-valued laser ring network. Fractals, 2023, 31(07): 2350091.

[9] Bao H, Wang Z, Hua Z, et al. Initial-Offset-Control Coexisting Hyperchaos in Two-Dimensional

Discrete Neuron Model. IEEE Transactions on Industrial Informatics, 2023, 20(3): 4784-4794.

[10] Yu F, Kong X, Yao W, et al. Dynamics analysis, synchronization and FPGA implementation of multiscroll Hopfield neural networks with non-polynomial memristor. Chaos, Solitons & Fractals, 2024, 179: 114440.

[11] Lin H, Wang C, Du S, et al. A family of memristive multibutterfly chaotic systems with multidirectional initial-based offset boosting. Chaos, Solitons & Fractals, 2023, 172: 113518.

[12] Volos C. Symmetry in Chaotic Systems and Circuits. Symmetry, 2022, 14(8): 1612.

[13] Li C, Lu T, Chen G, et al. Doubling the coexisting attractors. Chaos: An Interdisciplinary Journal of Nonlinear Science, 2019, 29(5): 051102 .

[14] Li C, Sprott J C, Xing H. Constructing chaotic systems with conditional symmetry. Nonlinear Dynamics, 2017, 87: 1351-1358.

[15] Li C, Xu Y, Chen G, et al. Conditional symmetry: Bond for attractor growing. Nonlinear Dynamics, 2019, 95: 1245-1256.

[16] Lin H, Wang C, Cui L, et al. Brain-like initial-boosted hyperchaos and application in biomedical image encryption. IEEE Transactions on Industrial Informatics, 2022, 18(12): 8839-8850.

[17] Li C, Sprott J C, Hu W, et al. Infinite multistability in a self-reproducing chaotic system. International Journal of Bifurcation and Chaos, 2017, 27(10): 1750160.

[18] Lin H, Wang C, Yu F, et al. A triple-memristor hopfield neural network with space multi-structure attractors and space initial-offset behaviors. IEEE Transactions on Computer-Aided Design of Integrated Circuits and Systems, 2023, 42(12): 4948-4958.

[19] Lai Q, Yang L, Hu G, et al. Constructing Multiscroll Memristive Neural Network With Local Activity Memristor and Application in Image Encryption. IEEE Transactions on Cybernetics, 2024, 54(7): 4039-4048.

[20] Bao H, Ding R, Liu X, et al. Memristor-cascaded Hopfield neural network with attractor scroll growth and STM32 hardware experiment. Integration, 2024, 96: 102164.

[21] Li Y, Li C, Liu S, et al. A 2-D conditional symmetric hyperchaotic map with complete control. Nonlinear Dynamics, 2022, 109: 1155-1165.

[22] Li C, Yi C, Li Y, et al. Offset boosting in a discrete system. Chaos: An Interdisciplinary Journal of Nonlinear Science, 2024, 34(3): 031102.

[23] Holmes P. A nonlinear oscillator with a strange attractor. Philosophical Transactions of the

Royal Society of London. Series A, Mathematical and Physical Sciences, 1979, 292(1394): 419-448.